Electronic Supplementary Material (ESI) for Journal of Materials Chemistry A.

Supporting information

Boost-up Electrochemical Performance of MOFs via Confined Synthesis within Nanoporous Carbon Matrices for Supercapacitor and Oxygen Reduction Reaction Applications

Hee Soo Kim[a], Min Seok Kang[a], and Won Cheol Yoo[a, b*]

[a]Department of Applied Chemistry, Hanyang University, 55 Hanyangdaehak-ro, Sangnok-gu, Ansan, Gyeonggi-do, 15588, Republic of Korea

[b]Department of Chemical and Molecular Engineering, Hanyang University, 55 Hanyangdaehak-ro, Sangnok-gu, Ansan, Gyeonggi-do, 15588, Republic of Korea

Corresponding Author*

e-mail: wcyoo@hanyang.ac.kr

Note 1. Calculation of the MOF volume fraction inside CM

For the following calculations, values listed in the Table 1 are used.

1. Densities of the pristine MOFs used for this work

Assumptions

1. We assume that the formula of HKUST-1 (Cu & Ni) are [$Cu_3(btc)_2$] and [$Ni_3(btc)_2$], respectively.

2. The crystallographic density (0.96 g/cc) of [$Cu_3(btc)_2(H_2O)_3$] reported in the paper (Chui et al. Science 1999, 283, 1148) is used for obtaining the following densities of Cu-/Ni-MOFs.

3. Molecular weights: [$Cu_3(btc)_2$] = 604.62 g/mol; [$Cu_3(btc)_2(H_2O)_3$] = 658.62 g/mol; [$Ni_3(btc)_2$] = 590.07 g/mol

- Density of [$Cu_3(btc)_2$]: 0.88 g/cc

The molecular weight ratio of [$Cu_3(btc)_2$] and [$Cu_3(btc)_2(H_2O)_3$] is 0.918 (604.62 g/mol / 658.62 g/mol), so the density for [$Cu_3(btc)_2$] is 0.88 g/cc (0.96 g/cc × 0.918)

- Density of [$Ni_3(btc)_2$]: 0.86 g/cc

The molecular weight ratio of [$Ni_3(btc)_2$] and [$Cu_3(btc)_2$] is 0.976 (590.07 g/mol / 604.62 g/mol), so the density for [$Ni_3(btc)_2$] is 0.86 g/cc (0.88 g/cc × 0.976)

2. Calculation of density of MC, NMC and mC

Assumptions

1. The density of solid carbon is assumed to be 2 g/cc (usually 1.8–2.1 g/cc).
2. Silica particles are packed in a *fcc* array (packing density = 74%).
3. The size of silica spheres is assumed to be uniform.
4. The density of air at 25 °C is 0.00118 g/cc.
5. The information of porosity for CMs can be obtained from nitrogen-sorption measurements.

► CMs contain 74% free volume, which is filled with air at ambient condition; this is because they are the inverse structure of the close-packed silica templates. The carbon content (the inverse *fcc*) is 26% in the CMs. Therefore, the density of CMs without considering microporosity is

$(0.26 \times 2\ g/cc) + (0.74 \times 0.00118\ g/cc) = 0.52\ g/cc$,

So, CM 1g = 1.923 cc.

► The microporosity of carbon should be considered for density.

- Volume fraction of MC within inverse *fcc* (microporosity = 0.15 cc/g): 92.2%

→ $(0.15\ cc / 1.923\ cc) \times 100 = 7.8\%$ for empty space of carbon due to microporoes, so volume fraction of carbon is 92.2%.

- Volume fraction of NMC within inverse *fcc* (microporosity = 0.11 cc/g): 94.3%

→ $(0.11\ cc / 1.923\ cc) \times 100 = 5.7\%$ for empty space of carbon due to microporoes, so volume fraction of carbon is 94.3%.

- Volume fraction of mC within inverse *fcc* (microporosity = 0.04 cc/g): 97.9%

→ $(0.04\ cc / 1.923\ cc) \times 100 = 2.1\%$ for empty space of carbon due to microporoes, so volume fraction of carbon is 97.9%.

- Density of MC: 0.48 g/cc

: $(0.26 \times 0.922 \times 2\ g/cc) + (0.26 \times 0.078 \times 0.00118\ g/cc) + (0.74 \times 0.00118\ g/cc) = 0.48\ g/cc$

- Density of NMC: 0.49 g/cc

: $(0.26 \times 0.943 \times 2\ g/cc) + (0.26 \times 0.057 \times 0.00118\ g/cc) + (0.74 \times 0.00118\ g/cc) = 0.49\ g/cc$

- Density of mC: 0.51 g/cc

: $(0.26 \times 0.979 \times 2\ g/cc) + (0.26 \times 0.021 \times 0.00118\ g/cc) + (0.74 \times 0.00118\ g/cc) = 0.51\ g/cc$

3. Calculation of the MOF volume fraction inside CMs using the micropore volume

Cu-MOF: density (0.88 g/cc) and micropore volume (0.49 cc/g)

Ni-MOF: density (0.86 g/cc) and micropore volume (0.3 cc/g)

MC: density (0.48 g/cc) and micropore volume (0.15 cc/g)

NMC: density (0.49 g/cc) and micropore volume (0.11 cc/g)

mC: density (0.51 g/cc) and micropore volume (0.04 cc/g)

Cu-MOF@MC-1: micropore volume (0.28 cc/g)

Cu-MOF@MC-2: micropore volume (0.33 cc/g)

Cu-MOF@NMC: micropore volume (0.32 cc/g)

Cu-MOF@mC: micropore volume (0.28 cc/g)

Ni-MOF@mC: micropore volume (0.17 cc/g)

► Considering that CMs have a free volume of 74% which can be occupied by a MOF, then the relative weights of MOF and CMs are follows

- In the 1 cc of Cu-MOF@MC, total weight = 0.651 + 0.125 = 0.776 g

Cu-MOF → 0.74 (cc, %) × 0.88 g/cc = 0.651 g (83.9%)

MC → 0.26 (cc, %) × 0.48 g/cc = 0.125 g (16.1%)

- In the 1 cc of Cu-MOF@NMC, total weight = 0.651 + 0.125 = 0.778 g

Cu-MOF → 0.74 (cc, %) × 0.88 g/cc = 0.651 g (83.7%)

NMC → 0.26 (cc, %) × 0.49 g/cc = 0.127 g (16.3%)

- In the 1 cc of Cu-MOF@mC, total weight = 0.651 + 0.133 = 0.784 g

Cu-MOF → 0.74 (cc, %) × 0.88 g/cc = 0.651 g (83%)

mC → 0.26 (cc, %) × 0.51 g/cc = 0.133 g (17%)

- In the 1 cc of Ni-MOF@mC, total weight = 0.636 + 0.133 = 0.769 g

Ni-MOF → 0.74% (cc) × 0.86 g/cc = 0.636 g (82.7%)

mC → 0.26% (cc) × 0.51 g/cc = 0.133 g (17.3%)

► If the entire free volume (74%) of CMs is occupied by MOF, then ideal micropore volumes of MOF@CMs are follows

- Cu-MOF@MC:
(0.839 × 0.49 cc/g) + (0.161 × 0.15 cc/g) = 0.435 cc/g

- Cu-MOF@NMC:
(0.837 × 0.49 cc/g) + (0.163 × 0.11 cc/g) = 0.428 cc/g

- Cu-MOF@mC:
(0.83 × 0.49 cc/g) + (0.17 × 0.04 cc/g) = 0.414 cc/g

- Ni-MOF@mC:
(0.827 × 0.3 cc/g) + (0.173 × 0.04 cc/g) = 0.255 cc/g

► Then, the relative micropore volume fractions of MOF inside CMs are follows
- Cu-MOF@MC-1 → (0.28 cc/g) / (0.435 cc/g) = 64.4%
- Cu-MOF@MC-2 → (0.33 cc/g) / (0.435 cc/g) = 75.9%
- Cu-MOF@NMC → (0.32 cc/g) / (0.428 cc/g) = 74.8%
- Cu-MOF@mC → (0.28 cc/g) / (0.414 cc/g) = 67.6%
- Ni-MOF@mC → (0.17 cc/g) / (0.255 cc/g) = 66.7%

4. Calculation of the MOF volume fraction inside CMs using TGA

Assumptions

1. Cu-/Ni-MOFs are transformed to CuO and NiO, respectively, and carbons are completely burned out during TGA measurement (air condition).
2. One mole of Cu-/Ni-MOFs ($[Cu_3(btc)_2]$ & $[Ni_3(btc)_2]$) gives three moles of CuO & NiO upon TGA measurement.
3. The volume fraction of MOF inside CM can be obtained from the relative weight ratio of MOF@CM sample and ideal weight of MOF@CM that a free volume (74%) of CM is completely occupied by MOF.
3. Molecular weights: $[Cu_3(btc)_2]$ = 604.62 g/mol; $[Ni_3(btc)_2]$ = 590.07 g/mol; CuO (MW): 79.54 g/mol; NiO (MW): 74.69 g/mol

► Considering that CMs have a free volume of 74%, which can be completely occupied by MOF, then the relative weights of MOF occupied in a free volume and MC are follows

- In the 1 cc of Cu-MOF@MC, total weight = 0.776 g

MC → 0.26 (cc, %) × 0.48 g/cc = 0.125 g (16.1%)

Cu-MOF → 0.74 (cc, %) × 0.88 g/cc = 0.651 g (83.9%) → 1.077×10^{-3} mol of $[Cu_3(btc)_2]$

→ 3.231×10^{-3} mol of CuO → (3.231×10^{-3} mol × 79.54 g/mol) = 0.257 g of CuO

So, the ideal leftover weight of Cu-MOF@MC when a free volume completely occupied by MOF after TGA is

0.257 / 0.776 = 33.1%

- In the 1 cc of Cu-MOF@NMC, total weight = 0.778 g

NMC → 0.26 (cc, %) × 0.49 g/cc = 0.127 g (16.3%)

Cu-MOF → 0.74 (cc, %) × 0.88 g/cc = 0.651 g (83.7%) → 1.077×10^{-3} mol of $[Cu_3(btc)_2]$

→ 3.231×10^{-3} mol of CuO → (3.231×10^{-3} mol × 79.54 g/mol) = 0.257 g of CuO

So, the ideal leftover weight of Cu-MOF@MC when a free volume completely occupied by MOF after TGA is

0.257 / 0.778 = 33%

- In the 1 cc of Cu-MOF@mC, total weight = 0.784 g

mC → 0.26 (cc, %) × 0.51 g/cc = 0.133 g (17%)

Cu-MOF → 0.74 (cc, %) × 0.88 g/cc = 0.651 g (83%) → 1.077 × 10^{-3} mol of [$Cu_3(btc)_2$]

→ 3.231 × 10^{-3} mol of CuO → (3.231 × 10^{-3} mol × 79.54 g/mol) = 0.257 g of CuO

So, the ideal leftover weight of Cu-MOF@MC when a free volume completely occupied by MOF after TGA is

0.257 / 0.784 = 32.8%

- In the 1 cc of Ni-MOF@mC, total weight = 0.636 + 0.133 = 0.769 g

mC → 0.26% (cc) × 0.51 g/cc = 0.133 g (17.3%)

Ni-MOF → 0.74% (cc) × 0.86 g/cc = 0.636 g (82.7%) → 1.078 × 10^{-3} mol mol of [$Cu_3(btc)_2$]

→ 3.234 × 10^{-3} mol of NiO → (3.234 × 10^{-3} mol × 74.69 g/mol) = 0.242 g of NiO

So, the ideal leftover weight of Cu-MOF@MC when a free volume completely occupied by MOF after TGA is

0.242 / 0.769 = 31.5%

► The relative weight fractions of MOF@CMs and ideal weights of MOF@CMs with a free volume completely occupied by MOF can be obtained using TGA data.

Cu-MOF@MC-1: 18.7% → 18.7 / 33.1 = 56.5%

Cu-MOF@MC-2: 25.7% → 25.7 / 33.1 = 77.6%

Cu-MOF@NMC: 24.7% → 24.7 / 33 = 74.8%

Cu-MOF@mC: 22.7% → 22.7 / 32.8 = 69.2%

Ni-MOF@mC: 18.5% → 18.5 / 31.5 = 58.7%

Note 2. Calculation of normalized capacitances (NCs) of MOFs

Assumptions

1. The capacitances of MOFs are boosted due to incorporation within conductive CMs.
2. The normalized capacitances of MOFs are obtained by considering the weight percentage of MOFs inside CMs.

- Cu-MOF@MC (77 F/g @0.3A/g): normalization capacitance (96 F/g @0.3A/g)

In the 1 cc of Cu-MOF@MC, actual volume fraction of Cu-MOF: 77.6%

Total weight: 0.63 g

MC → 0.26 (cc, %) × 0.48 g/cc = 0.125 g (19.8%)

Cu-MOF → 0.74 (cc, %) × 0.776 (%) × 0.88 g/cc = 0.505 g (80.2%)

Normalization factor: 1.247 (100 / 80.2), so 77 F/g × 1.247 = 96 F/g

- Cu-MOF@NMC (95 F/g @0.3A/g): normalization capacitance (119.8 F/g @0.3A/g)

In the 1 cc of Cu-MOF@NMC, actual volume fraction of Cu-MOF: 74.8%

Total weight: 0.614 g

NMC → 0.26 (cc, %) × 0.49 g/cc = 0.127 g (20.7%)

Cu-MOF → 0.74 (cc, %) × 0.748 × 0.88 g/cc = 0.487 g (79.3%)

Normalization factor: 1.261 (100 / 79.3) so, 95 F/g × 1.261 = 119.8 F/g

- Cu-MOF@mC (103 F/g @0.3A/g): normalization capacitance (132.6 F/g @0.3A/g)

In the 1 cc of Cu-MOF@mC, actual volume fraction of Cu-MOF: 69.2%

Total weight: 0.596 g

mC → 0.26 (cc, %) × 0.51 g/cc = 0.133 g (22.3%)

Cu-MOF → 0.74 (cc, %) × 0.692 × 0.88 g/cc = 0.463 g (77.7%)

Normalization factor: 1.287 (100 / 77.7) so, 103 F/g × 1.287 = 132.6 F/g

- Ni-MOF@mC: (103 F/g @ 0.3A/g): normalization capacitance (147.7 F/g @0.3A/g)

- In the 1 cc of Ni-MOF@mC, actual volume fraction of Cu-MOF: 58.7%

Total weight: 0.507 g

mC → 0.26% (cc) × 0.51 g/cc = 0.133 g (26.2%)

Ni-MOF → 0.74% (cc) × 0.587 × 0.86 g/cc = 0.374 g (73.8%)

Normalization factor: 1.355 (100 / 73.8) so, 109 F/g × 1.355 = 147.7 F/g

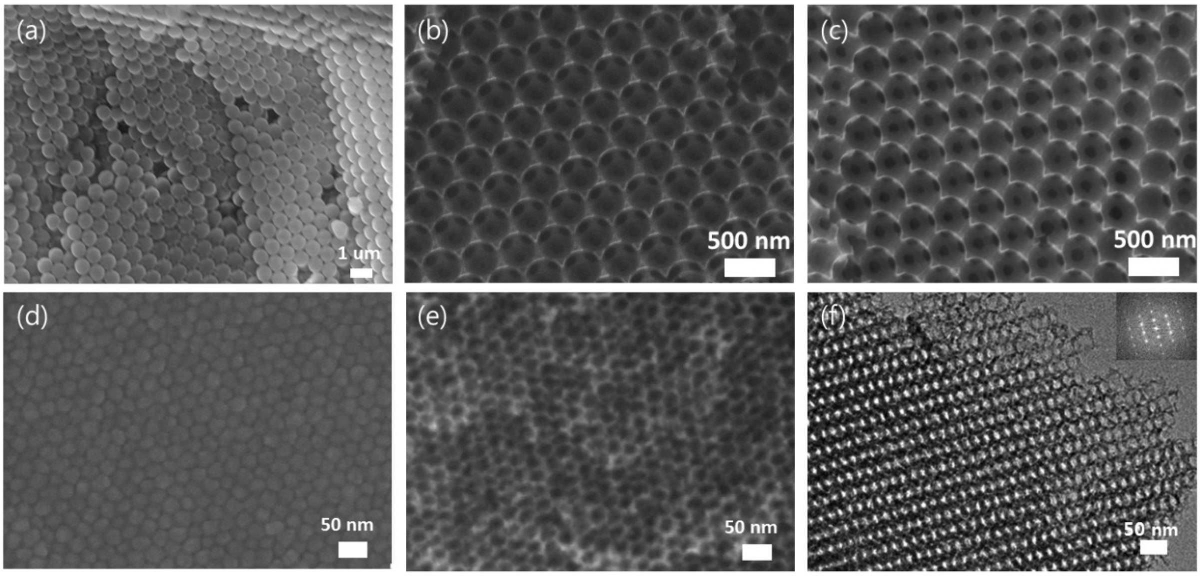

Figure S1. SEM images of PMMA colloidal crystal (a), MC (b), NMC (c), silica colloidal crystal (d), mC (d), and TEM image of mC (f) with corresponding FFT image (inset).

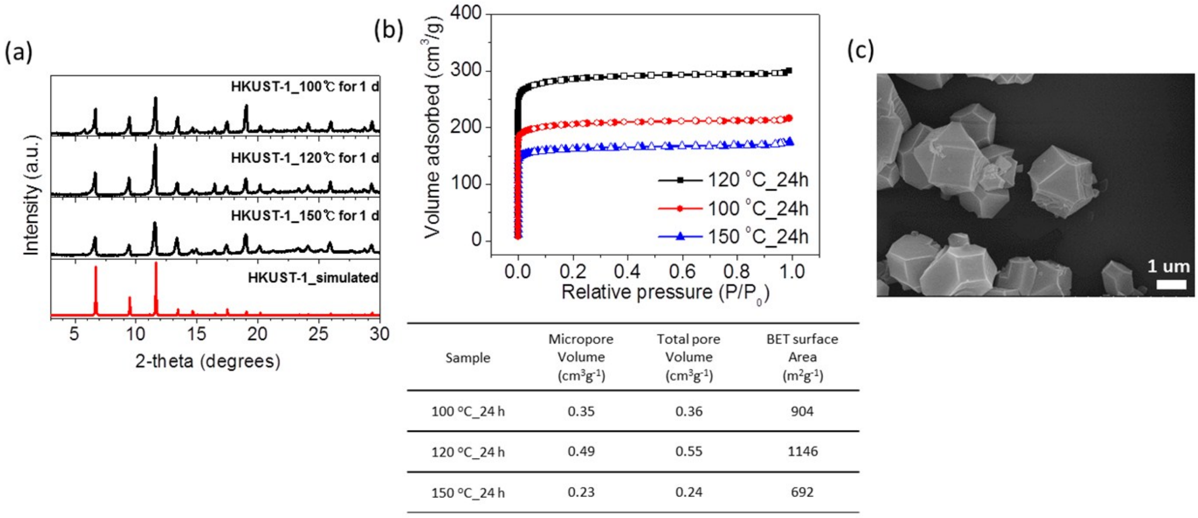

Sample	Micropore Volume (cm^3g^{-1})	Total pore Volume (cm^3g^{-1})	BET surface Area (m^2g^{-1})
100 °C_24 h	0.35	0.36	904
120 °C_24 h	0.49	0.55	1146
150 °C_24 h	0.23	0.24	692

Figure S2. Characterization of HKUST-1 synthesized by VAC process under different conditions (100, 120, and 150 °C for 24h): XRD results (a), N_2 sorption isotherms and corresponding textural features, and SEM image of Cu-MOF synthesized at 120 °C for 24h (c).

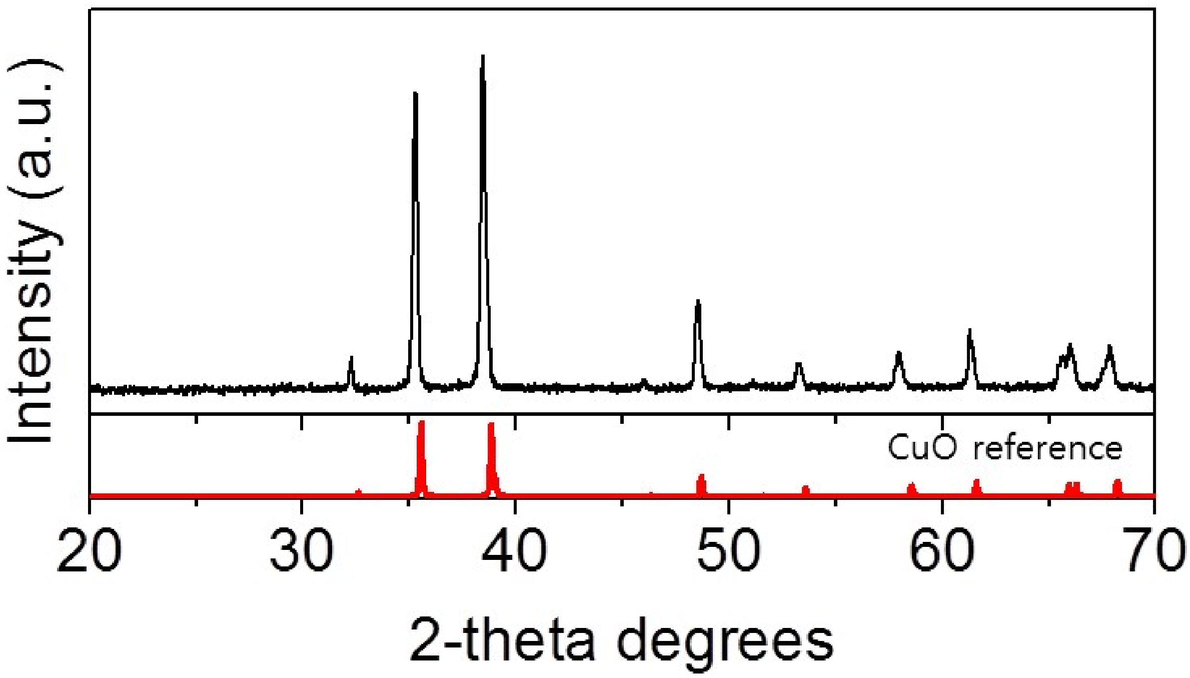

Figure S3. XRD data for leftover of Cu-MOF@MC after TGA measurement.

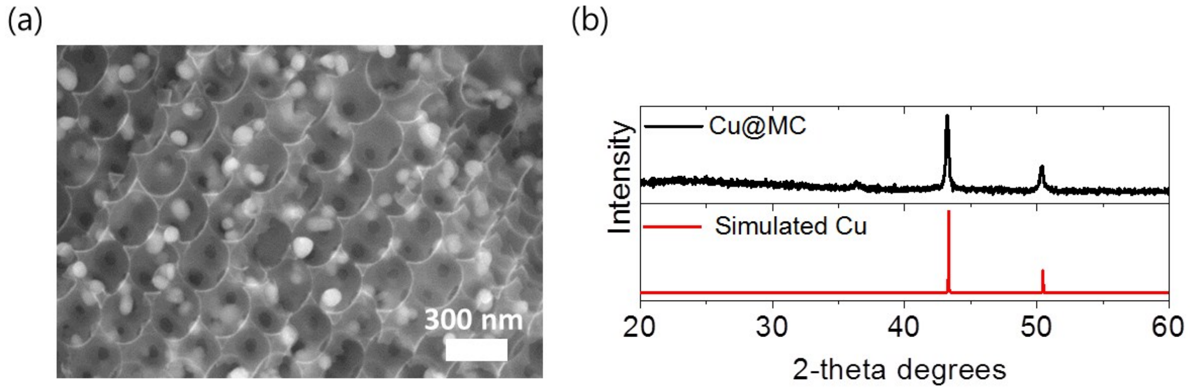

Figure S4. SEM image (a) and corresponding XRD data (b) of Cu@MC prepared through heat treatment of Cu-MOF@MC under N_2 atmosphere at 800 ℃ for 3h.

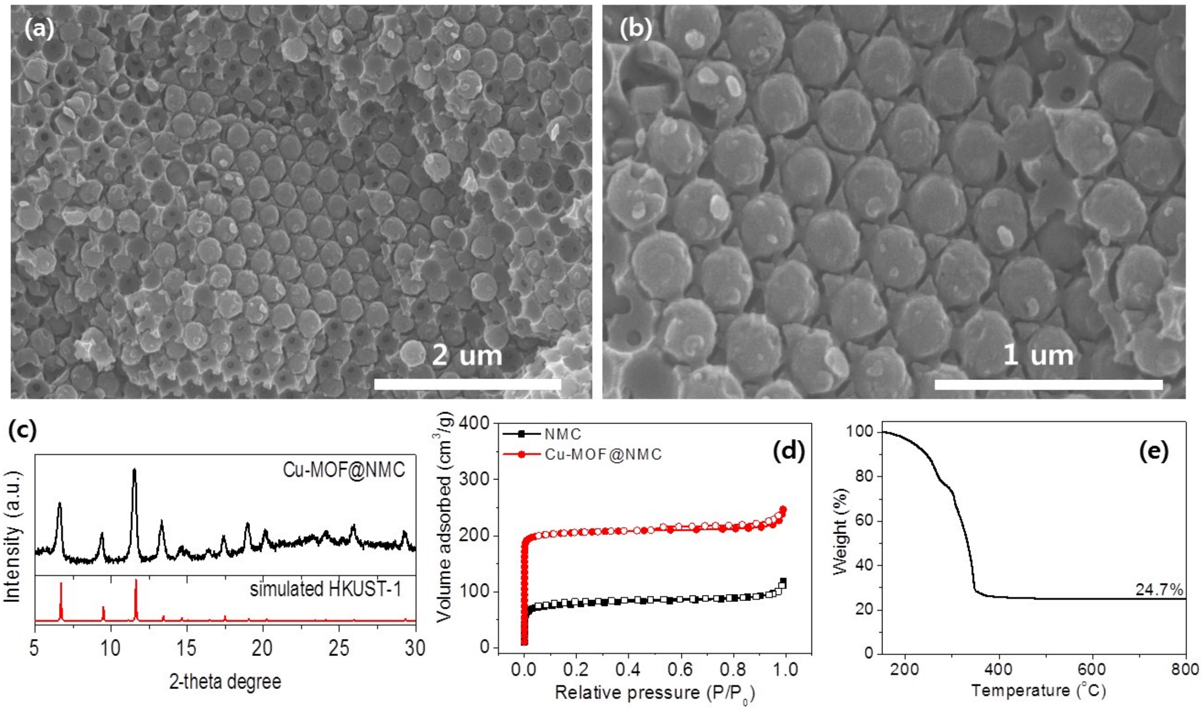

Figure S5. Characterization of Cu-MOF@NMC: low magnification (a) and enlarged (b) SEM images, XRD (c), N_2 sorption isotherms, and TGA result (e) of Cu-MOF@NMC.

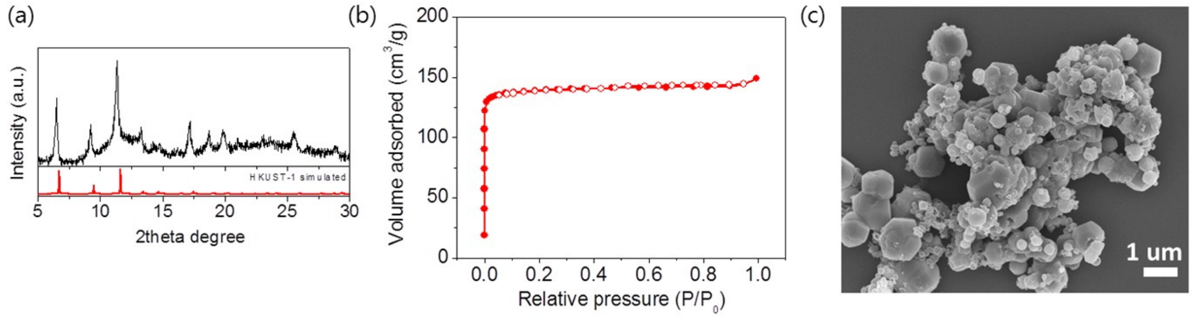

Figure S6. Characterization of Ni-MOF: XRD data (a), N_2 sorption isotherm (b), and SEM image (c) of Ni-MOF.

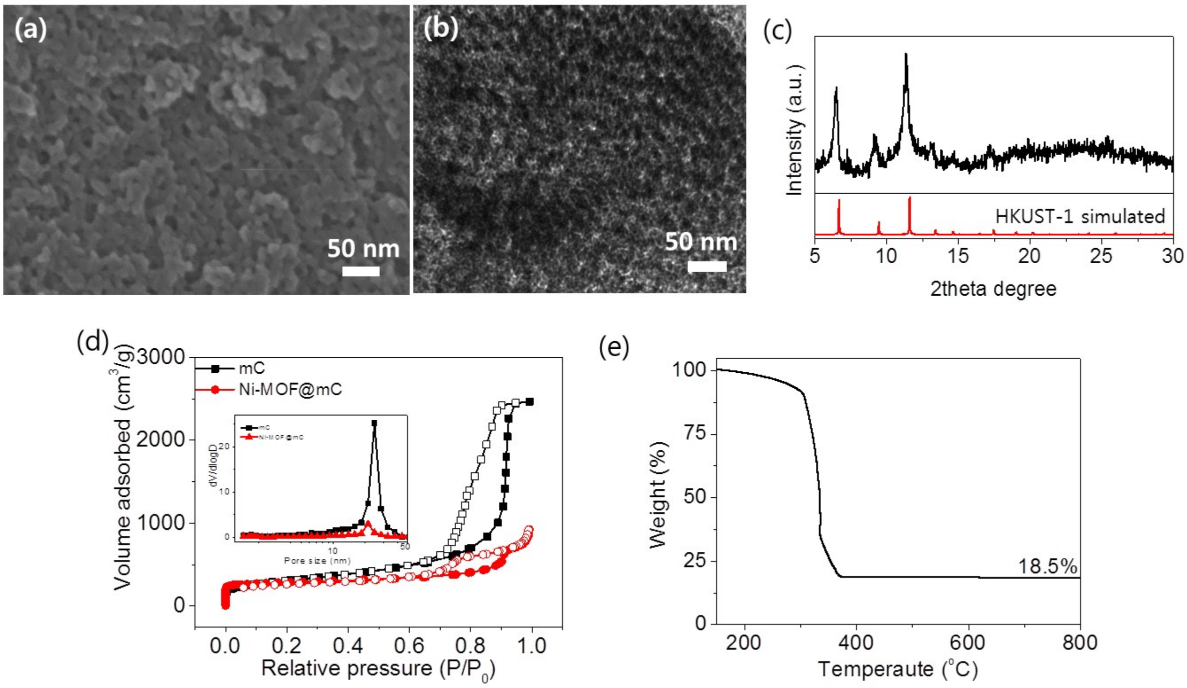

Figure S7. Characterization of Ni-MOF@mC: SEM (a) and TEM (b) images, XRD data (c), N_2 sorption isotherms (d), and TGA result (e) of Ni-MOF@mC.

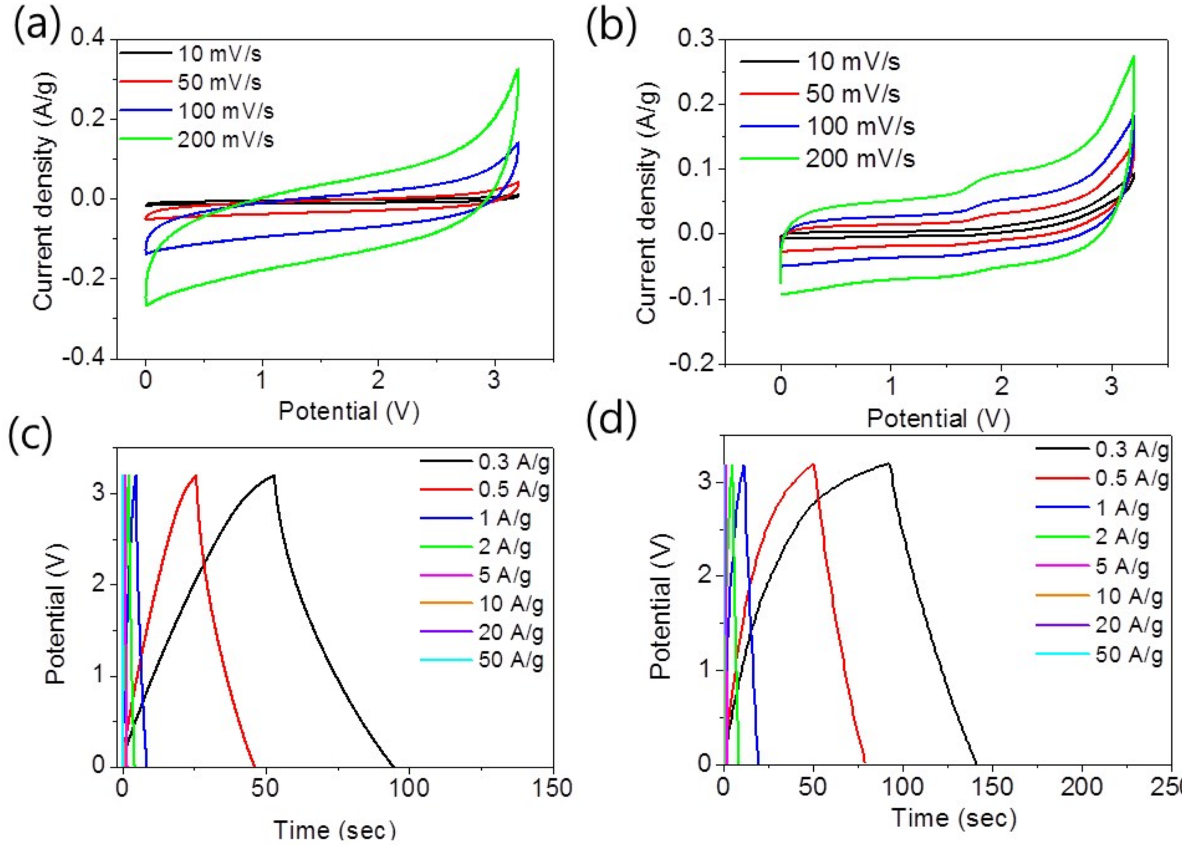

Figure S8. CV curves of Cu-MOF (a) and Ni-MOF (b) and charge-discharge curves of Cu-MOF (c) and Ni-MOF (d).

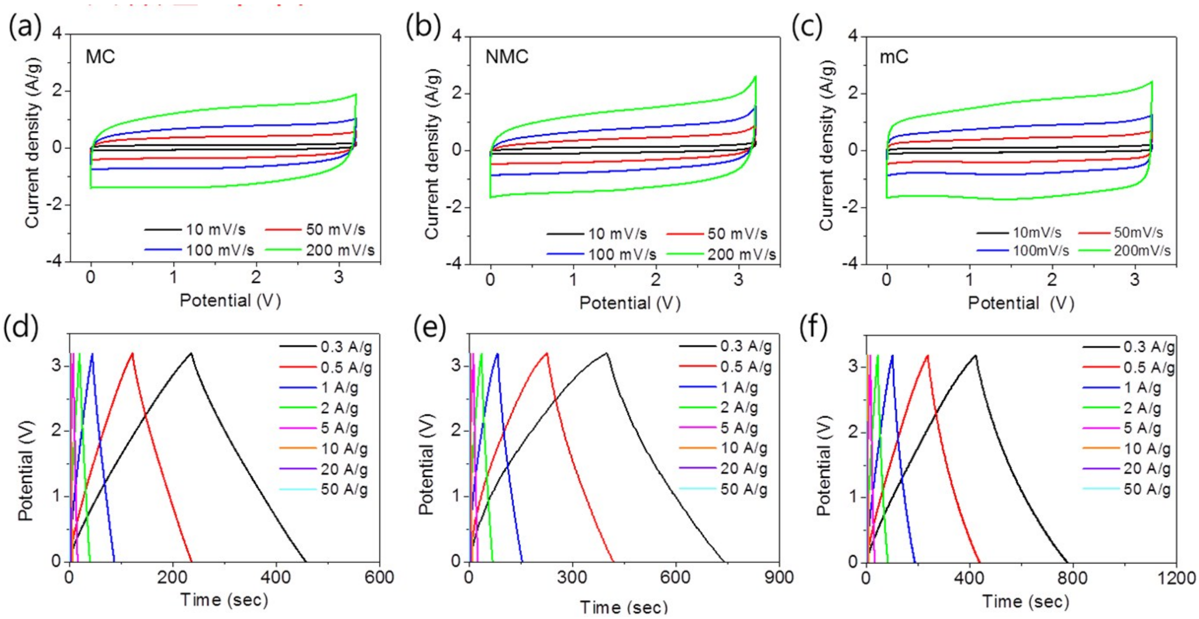

Figure S9. CV (a, b, and c) and charge-discharge (d, e, and f) curves of MC, NMC, and mC, respectively.

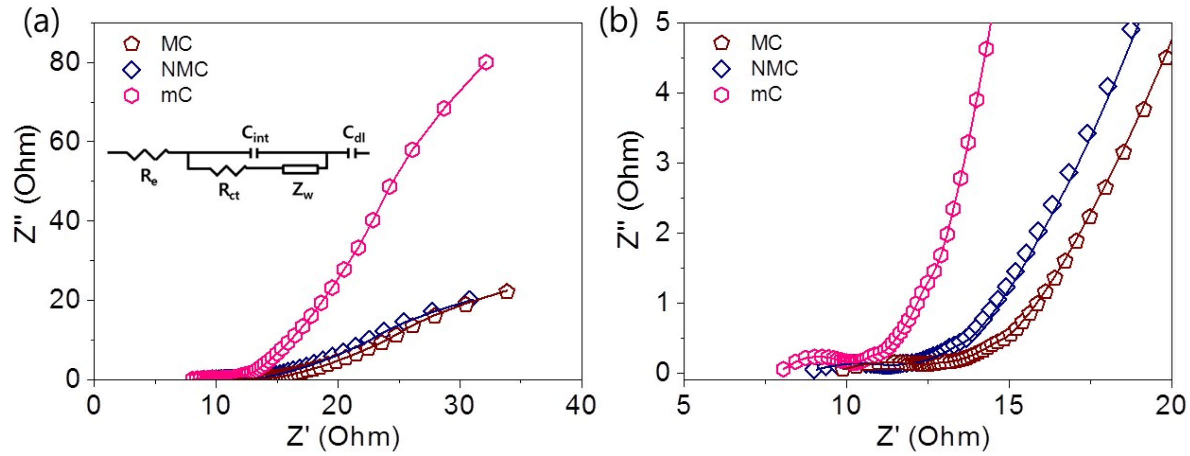

Figure S10. The Nyquist plots (a) of MC, NMC, and mC with inset of the equivalent circuit used for the fitting curves, and the details of Nyquist plots (b) in a high frequency range of MC, NMC, and mC.

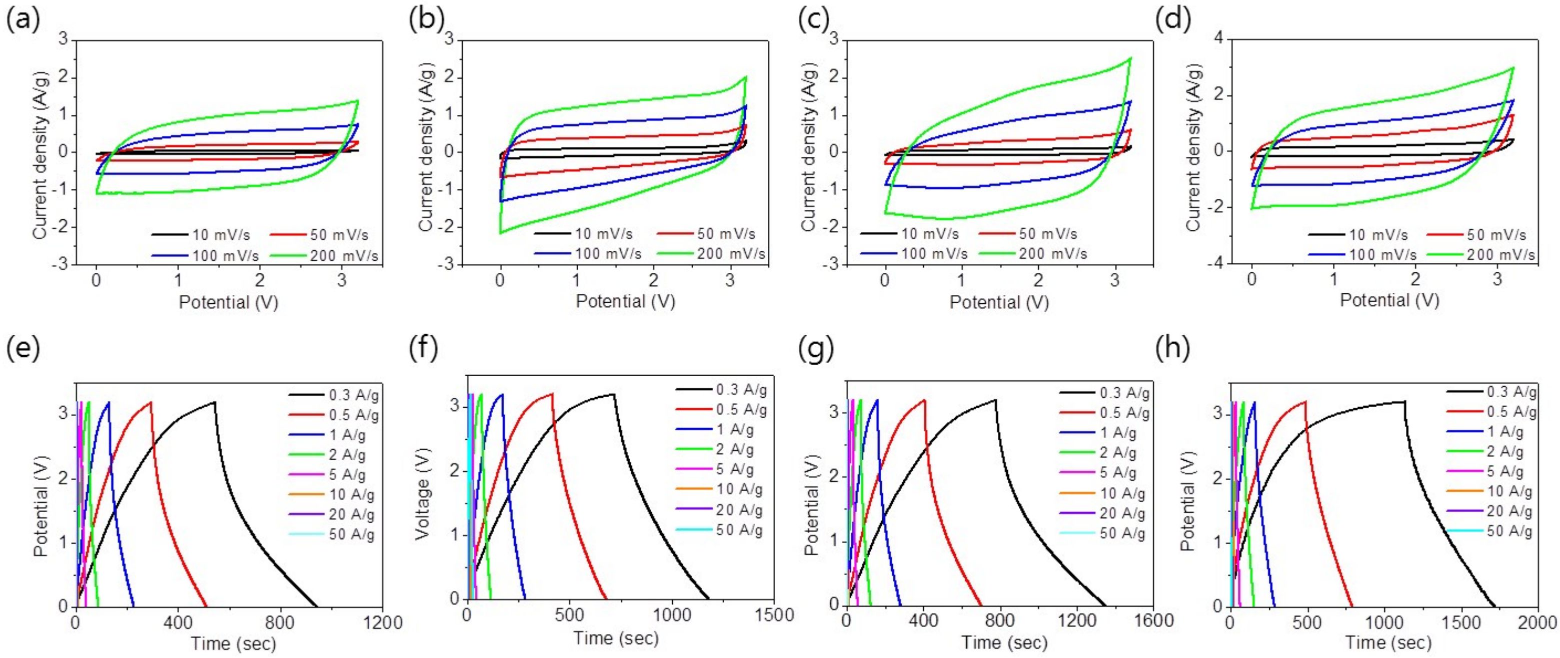

Figure S11. CV (a, b, c, and d) and charge-discharge (e, f, g, and h) curves of Cu-MOF@MC, Cu-MOF@NMC, Cu-MOF@mC, and Ni-MOF@mC, respectively.

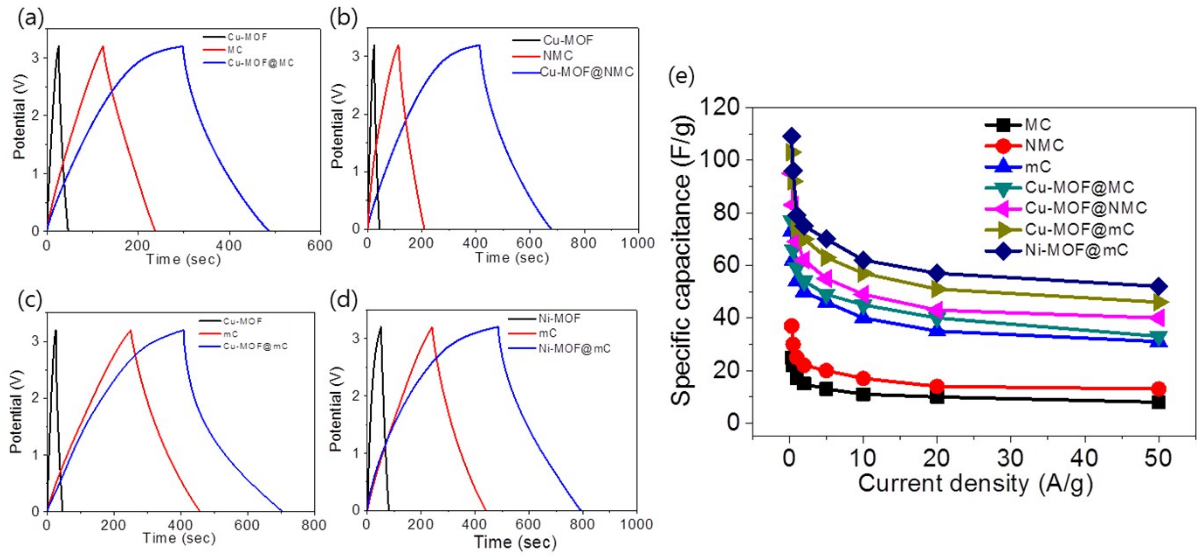

Figure S12. Charge-discharge profiles @0.5 A/g of a series of comparison groups such as Cu-MOF/MC/Cu-MOF@MC (a), Cu-MOF/NMC/Cu-MOF@NMC (b), Cu-MOF/mC/Cu-MOF@mC (c), and Ni-MOF/mC/Ni-MOF@mC (d), and capacity retention (e) at various current densities for CMs and MOF@CMs.

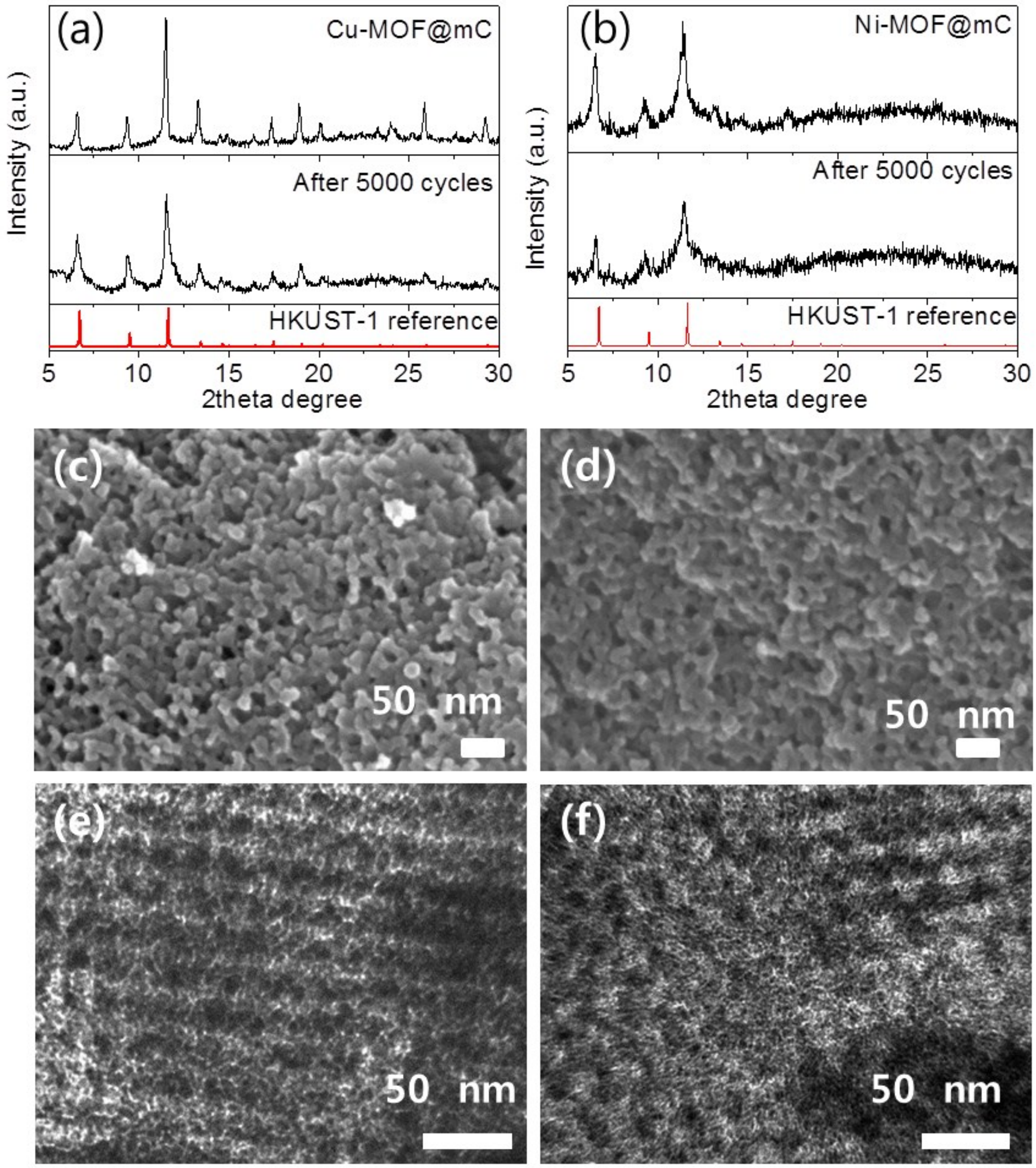

Figure S13. XRD (a), SEM (c) and TEM (e) images for Cu-MOF@mC, and XRD (b), SEM (d) and TEM (f) images for Ni-MOF@mC after 5000 cycles at current density of 5 A/g.

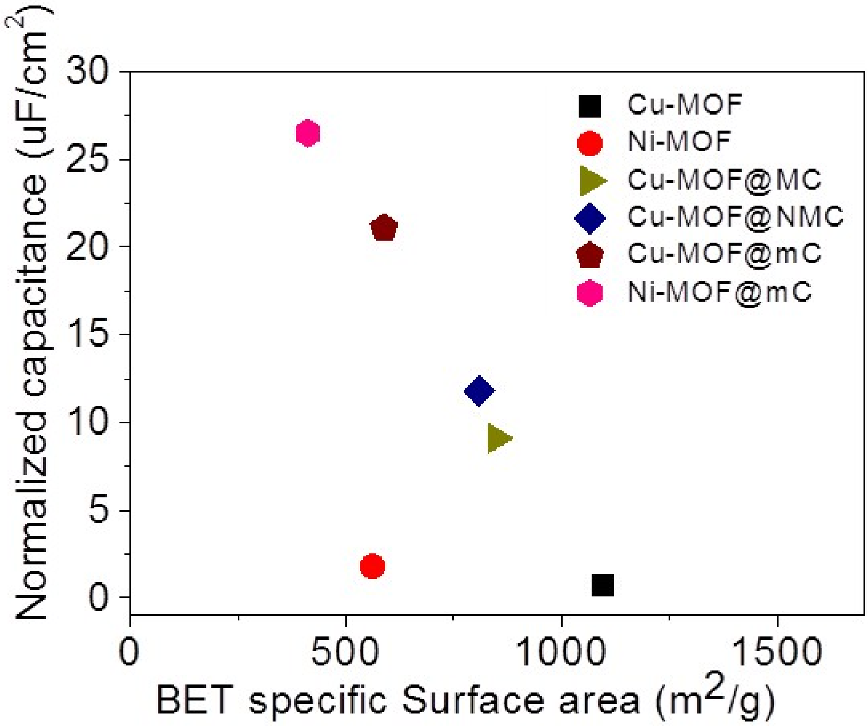

Figure S14. Comparison of SSA normalized capacitances of the pristine MOFs and MOF@CMs.

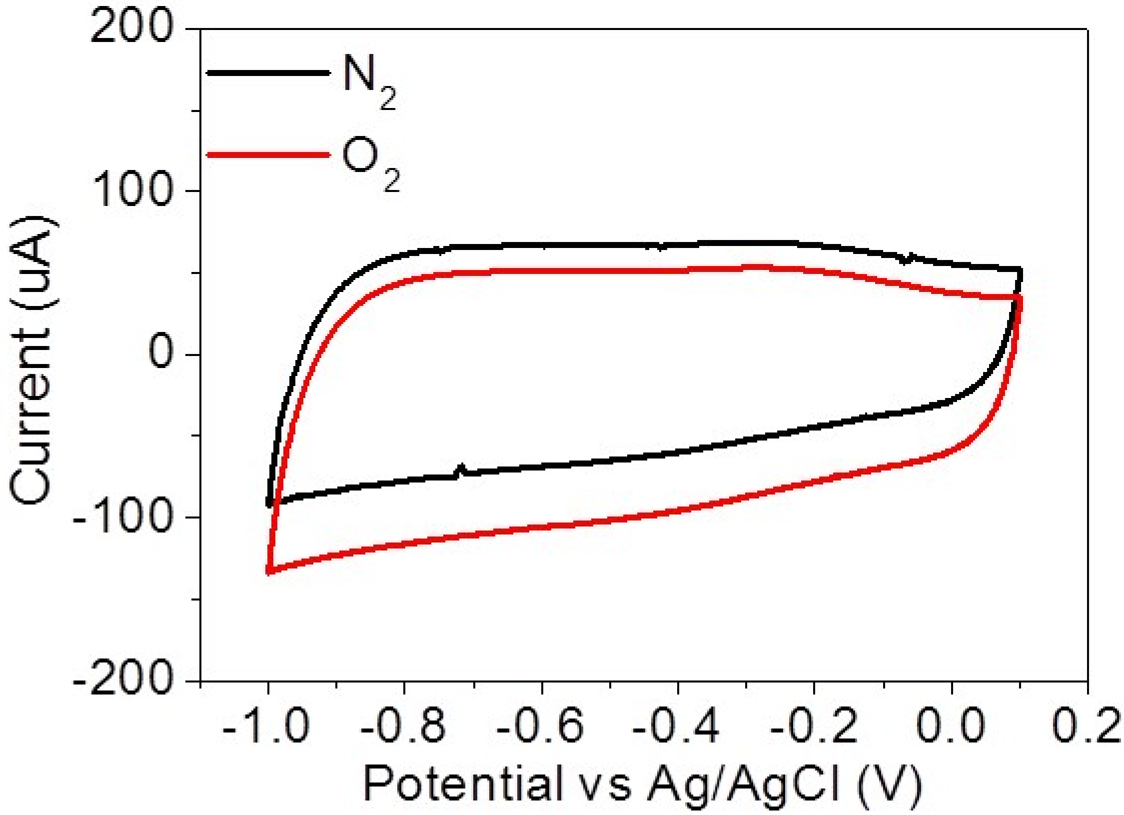

Figure S15. CV curves of mC under N_2 and O_2 saturated 0.1 M KOH solutions.

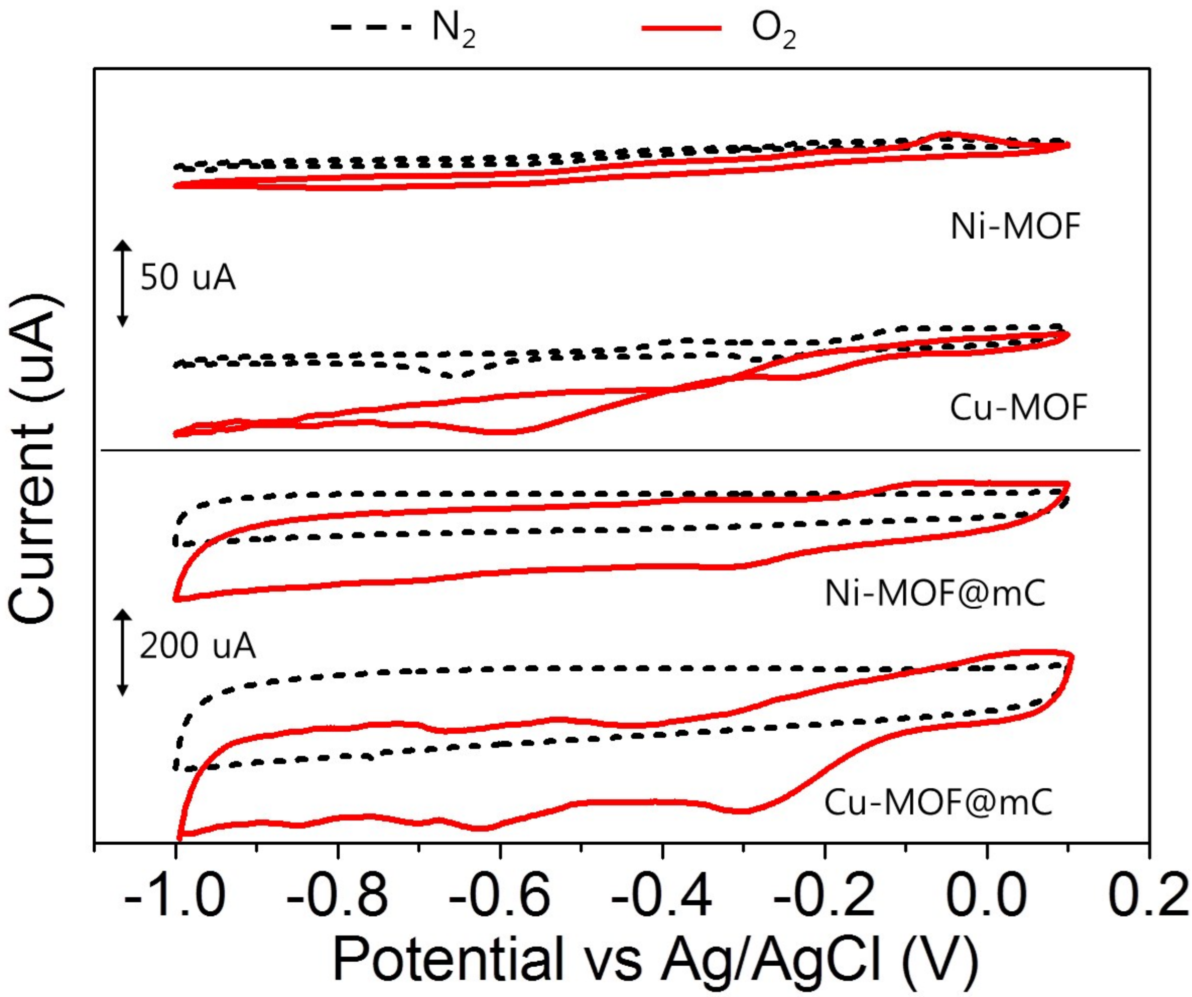

Figure S16. CV curves of the pristine MOFs and Cu-/Ni-MOF@mCs under N_2 and O_2 saturated 0.1 M KOH solutions.

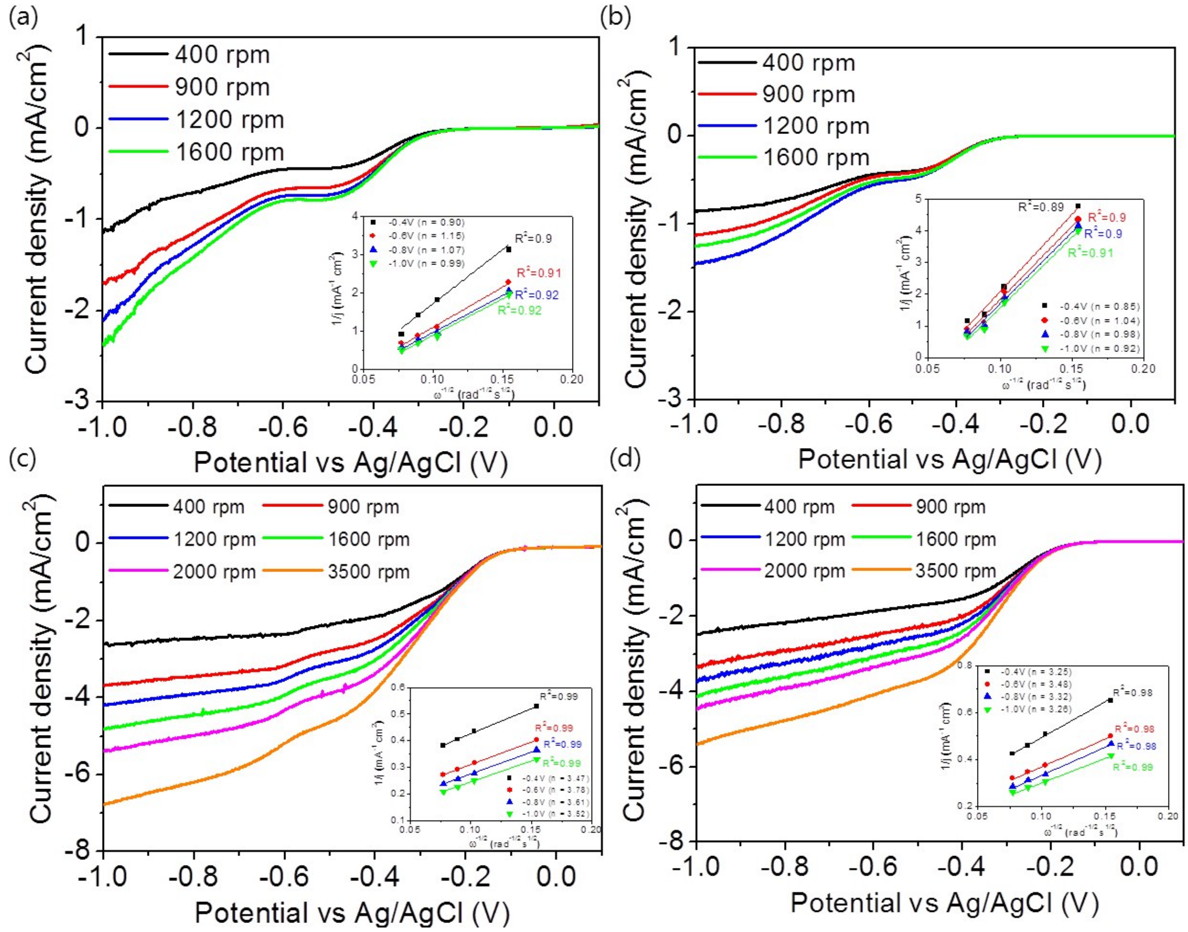

Figure S17. RDE polarization curves in O_2-saturated 0.1 M KOH with various scan rates of Cu-MOF (a), Ni-MOF (b), Cu-MOF@mC (c), and Ni-MOF@mC with insets of KL plots at various potentials vs. Ag/AgCl (V).

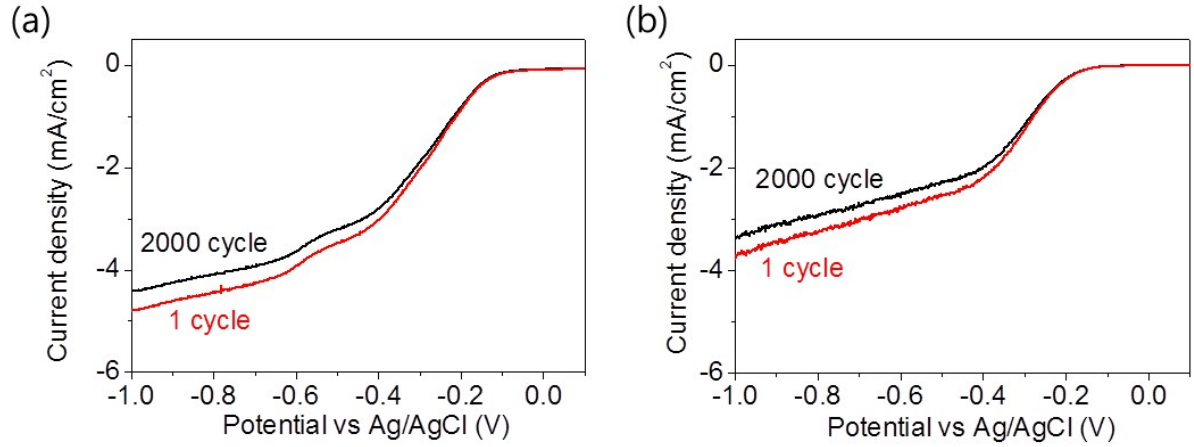

Figure S18. RDE polarization curves before/after 2000 cycles for Cu-MOF@mC (a) and Ni-MOF@mC (b).

Table S1. The supercapacitive performances of pristine MOFs, CMs, and MOF@CMs, and MOFs incorporated within CMs.

Sample	C@ 0.3 A/g (F/g) [a]	C@ 0.5 A/g (F/g)	C@ 1 A/g (F/g)	C@ 2 A/g (F/g)	C@ 5 A/g (F/g)	C@ 10 A/g (F/g)	C@ 20 A/g (F/g)	C@ 50 A/g (F/g)	Retention @50A/g (%)[b]	CE @50 A/g[c]
Cu-MOF	8	6	4	3	1.9	1.4	1	0.66	17	
Ni-MOF	10	9	5	4.3	3.1	2.1	1.5	0.92	18	
MC	25	22	17	15	13	11	10	8	47	
NMC	37	30	25	22	20	17	14	13	52	
mC	73	62	54	50	46	40	35	31	57	
Cu-MOF @MC	77	66	59	54	49	45	40	33	56	
Cu-MOF @NMC	95	83	69	62	55	49	43	40	58	
Cu-MOF @mC	103	92	74	70	63	57	51	46	62	
Ni-MOF @mC	109	96	79	75	70	62	57	52	66	
N-Cu-MOF @MC[d]	96	82	74	67	61	56	50	41		62
N-Cu-MOF @NMC[d]	120	105	87	78	69	62	54	50		76
N-Cu-MOF @mC[d]	133	118	95	90	81	73	66	59		89
N-Ni-MOF @mC[d]	148	130	107	102	95	84	77	70		76

[a]Gravimetric capacitance at various current densities; [b]Retention@50 A/g compared to capacitance@1A/g; [c]Capacity enhancement obtained from the ratio of normalized capacitance to weight content of MOF incorporated within CM and capacitance of pristine MOF; [d]MOF incorporated within CM; the values in the shaded area: normalized capacitances.

Table S2. Equivalent series resistance (R_e) and charge transfer resistance (R_{ct}) of the pristine MOFs, MCs, and MOF@CMs

Sample	Cu-MOF	Ni-MOF	MC	NMC	mC	Cu-MOF @MC	Cu-MOF @NMC	Cu-MOF @mC	Ni-MOF @mC
R_e (Ω)	12.1	11.9	9.8	8.2	7.6	7.7	6.02	3.8	3.73
R_{ct} (Ω)	-	-	3.1	2.9	2.47	2.1	1.4	0.9	0.82

Table S3. The supercapacitive performances of CMs, pristine MOFs, and MOF@CMs.

Sample	Normalized Capacitance (0.3 A/g, uF/cm^2)[a] (BET SSA, m^2/g)	Normalized Capacitance (50 A/g, uF/cm^2)[a] (BET SSA, m^2/g)	Maximum energy density (Wh/kg)	Maximum power density (W/kg)
MC	6.4 (391)	2.0 (391)	-	-
NMC	12.3 (302)	4.3 (302)	-	-
mC	6.6 (1107)	2.8 (1107)	-	-
Cu-MOF	0.7 (1146)	0.06 (1146)	2.8	2197
Ni-MOF	1.8 (561)	0.15 (561)	3.6	2520
Cu-MOF@MC	9.1 (848)	3.9 (848)	27.4	14388
Cu-MOF@NMC	11.8 (808)	4.7 (808)	33.8	15140
Cu-MOF@mC	21.1 (488)	9.4 (488)	36.6	19620
Ni-MOF@mC	26.5 (411)	12.7 (411)	38.8	21005

[a]Specific surface area (SSA) normalized capacitances.

Table S4. Comparison of the SSA normalized capacitances of Cu-/Ni-MOF@mCs and various EDLCs plotted in the Figure 4a.

Sample	BET surface Area (m^2/g)	Capacitance (F/g)	Normalized Capacitance (uF/cm^2)	Electrolyte	Ref
$Ni_3(HTTP)_2$	630	111 (0.05 A/g)	18	1M $TEABF_4$/ACN	Ref S1.
Cu-CAT NWA	540	202 (0.5 A/g)	22	3M KCl	Ref S2.
CDC	1850	140 (1 A/g)	7.6	6M KOH	Ref S3.
M-30	2298	121 (1 A/g)	5.3	1M $TEABF_4$/ACN	Ref S4.
DCG-5	1121	83 (1 A/g)	7.4	1M $TEABF_4$/ACN	Ref S4.
PC94-11ox	1165	78 (1 A/g)	4.6	1M $TEABF_4$/ACN	Ref S4.
KP-1500	1568	107 (1 A/g)	6.8	1M $TEABF_4$/ACN	Ref S4.
AC-700	1606	72 (0.1 A/g)	4.5	1M H_2SO_4	Ref S4.
Chemically reduced graphene	2400	165 (1.4 A/g)	7	1M $TEABF_4$/ACN	Ref S5.
SWNT arrays	1300	160 (1A/g)	12	1M $TEABF_4$/ACN	Ref S6.
Activated graphene	3523	202 (1A/g)	6	1M $TEABF_4$/ACN	Ref S7.
Holey Graphene	810	262 (1A/g)	32	$EMIMBF_4$/ACN	Ref S8.
N-A graphene	1542	84 (0.5A/g)	5.4	6M KOH	Ref S9.
PaGM-600	891	172 (0.2A/g)	19.3	$BMIMBF_4$	Ref S10.
Cu-MOF@mC	488	103 (0.3 A/g)	21.1	1M $TEABF_4$/ACN	In this work
Ni-MOF@mC	411	109 (0.3 A/g)	26.5	1M $TEABF_4$/ACN	In this work

Table S5. Comparison of supercapacitive performances of Cu-/Ni-MOF@mCs and various MOF-based EDLCs.

Sample	Max energy density	Max power density	Long-term cycle performance (%)	Reference
$Ni_3(HITP)_2$	2.4 Wh kg^{-1a}	2200 W kg^{-1a}	10000 cycle, 90%	Ref S1.
Cu-MOF-NWs	2.6 Wh/kg	3100 W/kg	5000 cycle, 85%	Ref S2.
nMOF-867	0.00385 mWh/cm^2	8.67 mW/cm^2	5.09	Ref S11.
HKUST/RGO	42 Wh/ kg	3100 W/ kg	4000 cycle. 99%	Ref S12.
CNTs@Mn-MOF	6.9 Wh/ kg	2240 W/ kg	3000 cycle, 88%	Ref S13.
ZIF-67/PANI	0.0161 mWh/cm^3 0.0044 mWh/cm^2	833 mW/cm^3 245 mW/cm^2	2000 cycle, 80%	Ref S14.
PEDOT/HKUST-1/Graphene/CNTF	0.0022 mWh/cm^2	0.2 mW/cm^2	1000 cycle, 80%	Ref S15.
ZIF−PPy	0.0113 mWh/cm^2	1.44 mW/cm^2	10000 cycle, 91%	Ref S16.
Cu-MOF@mC	36.6 Wh/kg 0.0395 mWh/cm^{2b}	19620 W/ kg 21 mW/cm^{2b}	5000 cycle, 91%	In this work
Ni-MOF@mC	38.8 Wh/kg 0.042 mWh/cm^{2b}	21005 W/ kg 23 mW/cm^{2b}	5000 cycle, 91%	In this work

[a]Gravimetric maximum energy and power densities calculated according to the reported values; [b]Electrode area obtained as follows: $\pi (0.55)^2 = 0.95\ cm^2 \times 2$ (symmetric cell) $= 1.9\ cm^2$

Table S6. Comparison of ORR activities of our Cu-/Ni-MOF@mCs and MOF-based ORR electrocatalysts.

Sample (RDE measurement)	Onset Potential (V vs. Ag/AgCl)[a]	Half-wave Potential (V vs. Ag/AgCl)[a]	Maximum Current Density (mA/cm^2)	Maximum Electron Transfer Number	Ref
(G-dye 50wt%-FeP)$_n$MOF (2000 rpm)	-	- 0.5	6.2	3.82	Ref S17.
(GO 8wt%)Cu.MOF (3500 rpm)	- 0.67	- 1.16	5.32	3.95	Ref S18.
MOF(Fe/Co) (1600 rpm)	- 0.13	- 0.7	3.9	4.0	Ref S19.
$Ni_3(HITP)_2$ (2000 rpm)	- 0.144	- 0.26	2.5	2.25	Ref S20.
Ni/Co-MOF (1600rpm)	- 0.204	- 0.41	4.51	3.7	Ref S21.
Ɛ-MnO_2/MOF(Fe) (1600 rpm)	- 0.12	- 0.324	5.56	3.9	Ref S22.
Ni-MOF@mC (3500 rpm)	- 0.101	- 0.38	5.4	3.48	In this work
Cu-MOF@mC (3500 rpm)	- 0.091	- 0.36	6.8	3.78	In this work

[a]Onset and half-wave potentials of references converted to potentials vs. Ag/AgCl using the following relationship of Ag/AgCl (V) + 0.0964 = RHE.

References

[S1]. D. Sheberla, J. C. Bachman, J. S. Elias, C. J. Sun, Y. Shao-Horn and M. Dincă, *Nat. Mater.,* 2017, **16**, 220-224.

[S2]. W. H. Li, K. Ding, H. R. Tian, M. S. Yao, B. Nath, W. H. Deng, Y. Wang and G. Xu, *Adv. Funct. Mater.,* 2017, **27**, 1702067.

[S3]. J. Chmiola, G. Yushin, Y. Gogotsi, C. Portet, P. Simon and P.-L. Taberna, *Science*, 2006, **313**, 1760-1763.

[S4]. T. A. Centeno and F. Stoeckli, *Electrochim. Acta,* 2011, ***56***, 7334-7339

[S5]. Y. Zhu, S. Murali, M. D. Stoller, K. J. Ganesh, W. Cai, P. J. Ferreira, A. Pirkle, R. M. Wallace, K. A. Cychosz, M. Thommes, D. Su, E. A. Stach and R. S. Ruoff, *Science,* 2011, **332**, 1537-1541.

[S6]. A. Izadi-Najafabadi, S. Yasuda, K. Kobashi, T. Yamada, D. N. Futaba, H. Hatori, M. Yumura, S. Iijima and K. Hata, *Adv. Mater.,* 2010, ***22***, E235-E242

[S7] G. Zhang and X. W. D. Lou, *Sci. Rep*. 2013, ***3***, 1408-1417.

[S8]. Y. Xu, Z. Lin, X. Zhong, X. Huang, N. O. Weiss, Y. Huang and X. Duan, *Nat. Commun.,*2014, **5**, 4554-4562.

[S9]. Z. Chen, K. Liu, S. Liu, L. Xia, J. Fu, X. Zhang, C. Zhang and B. Gao, *Electrochim. Acta,* 2017, ***237***, 102-108.

[S10]. H. Li, Y. Tao, X. Zheng, J. Luo, F. Kang, H.-M. Cheng and Q.-H. Yang, *Energy Environ. Sci.* 2016, **9**, 3135-3142.

[S11]. K. M. Choi, H. M. Jeong, J. H. Park, Y.-B. Zhang, J. K. Kang and O. M. Yaghi, *ACS Nano,* 2014, **8**, 7451-7457.

[S12]. P. Srimuk, S. Luanwuthi, A. Krittayavathananon and M. Sawangphruk, *Electrochimica. Acta,* 2015, **157**, 69-77.

[S13]. Y. Zhang, B. Lin, Y. Sun, X. Zhang, H. Yang and J. Wang, *RSC Adv.,* 2015, **5**, 58100-58106.

[S14]. L. Wang, X. Feng, L. Ren, Q. Piao, J. Zhong, Y. Wang, H. Li, Y. Chen and B. Wang, *J. Am. Chem. Soc.,* 2015, **137**, 4920-4923.

[S15]. D. Fu, H. Zhou, X.-M. Zhang, G. Han, Y. Chang and H. Li, *ChemistrySelect,* 2016, **1**, 285-289.

[S16]. X. Xu, J. Tang, H. Qian, S. Hou, Y. Bando, M. S. A. Hossain, L. Pan and Y. Yamauchi,

ACS Appl. Mater. Interfaces, 2017, **9**, 38737-38744.
[S17]. M. Jahan, Q. Bao and K. P. Loh, *J. Am. Chem. Soc.,* 2012, **134**, 6707-6713.
[S18]. M. Jahan, Z. Liu and K. P. Loh, *Adv. Funct. Mater.,* 2013, **23**, 5363-5372.
[S19]. H. Wang, F. Yin, G. Li, B. Chen and Z. Wang, *Int. J. Hydrogen Energy,* 2014, ***39***, 16179-16186.
[S20]. E. M. Miner, T. Fukushima, D. Sheberla, L. Sun, Y. Surendranath and M. Dincă, *Nat. Commun.,* 2016, **7**, 10942-10949.
[S21]. H. Xia, J. Zhang, Z. Yang, S. Guo, S. Guo and Q. Xu, *Nano-Micro Lett.* 2017, ***9***, 43-54.
[S22]. H. Wang, F. Yin, B. Chen and G. Li, *J. Mater. Chem. A,* 2015, ***3***, 16168-16176.